# Scrape off layer transport in MAST L-mode plasma: the role of instability

D. Higgins[1], B. Hnat[1], A. Kirk[2], P. Tamain[2,3], N. Ben Ayed[2] and the MAST team

[1] CFSA, Department of Physics, Warwick University, Coventry CV4 7AL, UK
[2] EURATOM/CCFE, Culham Science Centre, Abingdon, Oxon, OX14 3DB, UK
[3] Present address: CEA-IRFM, F-13108 Saint-Paul-lez-Durance, France.

## Filament Model Theory

### Interchange Mechanism

- A large fraction ($\approx 1$) of fluxes entering SOL can flow to the main wall and not the divertor [**2**].
- The interchange mechanism is responsible for the radial convection of coherent structures [**3**]

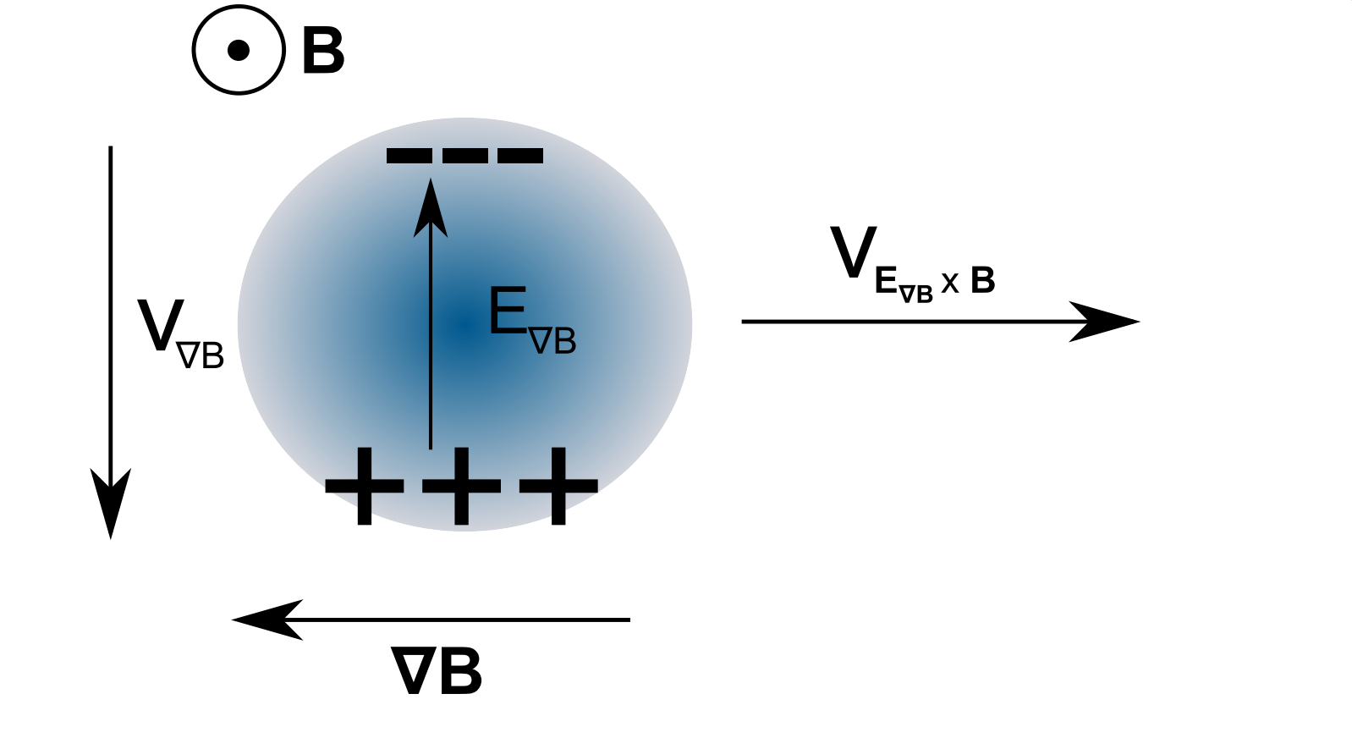

$$V_{\nabla B} = 1/qB^3\ (\mathbf{B} \times \nabla\mathbf{B})$$

$$V_{E_{\nabla B} \times B} = (\mathbf{E} \times \mathbf{B})/B^2$$

*Schematic model of filament $E \times B$ advection, from a guiding centre drift perspective.*

### Sheath dissapative interchange drive

- Parrallal sheath currents arrise in maintaining a positive sheath at the divertor [**7**].
- This is a dissapation driven by a potential in the midplane.
- In the steady state where $\nabla \cdot J = 0$, the potential inside the filament can be found [**3**].

$$\vec{\nabla}_{\|}\left[en_tC_s\left(\frac{e\phi}{T}\right)\right] = -\vec{\nabla}_{\perp}\cdot\left[\frac{T}{B^2}\left(\vec{B}\times\vec{\nabla}\,n_b\right)\right]$$

$$\frac{e\phi}{T} = \left(\frac{l_b\rho_i}{2Rn_t}\right)\frac{\partial n_b}{\partial y}$$

$$v_r = C_s\frac{l_b}{R}\left(\frac{\rho_i}{\delta}\right)^2\frac{n_b}{n_t}$$

In these limits a radial advection velocity for the filament solution is found, with the sheath dissapation balancing the interchange drive.

### Nonlinear interchange drive

Balancing the interchange drive with the polarisation current leads to the field aligned component of the vorticity equation, ignoring the parallel sheath dissapation.

$$\vec{\nabla}\cdot m\frac{d\vec{E}}{dt} = \vec{\nabla}\cdot\frac{\vec{B}\times\vec{\nabla}p}{n}$$

$$\left(\partial_t + \hat{z}\times\vec{\nabla}\phi\cdot\vec{\nabla}\right)\Omega + \frac{\partial\tilde{n}}{\partial y} = \mu\vec{\nabla}_{\perp}^2\Omega$$

$$v_r \sim C_s\left(\frac{2l}{R}\frac{\Delta\tilde{n}}{n_0}\right)^{\frac{1}{2}}$$

The filament ExB velocity scaling is found via dimensional analysis of the vorticity equation.

## Motivation

- The fast transport of plasma toward plasma facing components via convective motions of filaments is a challenge for next step tokamak fusion reactors.
- This transport places limits on the life cycle of plasma facing components, and creates a source of radioactive dust in the reaction chamber [8].
- These affects must be accounted for in the operational cycle, and crucially will affect the operational feasaability of the device [1].
- Here a comparison of models for interchange motions of isolated blobs is made for data from the MAST tokamak and simulated data.

## Data Analysis

### Overview

- Data is taken from the Guendestrup probe system mounted on a reciprocating head.
- This provides measurments of the plasma floating potential and the ion saturation current over the radial motion of the probe.
- Data from a $D_\alpha$ emmision camera is used to estimate the position of the LCFS.

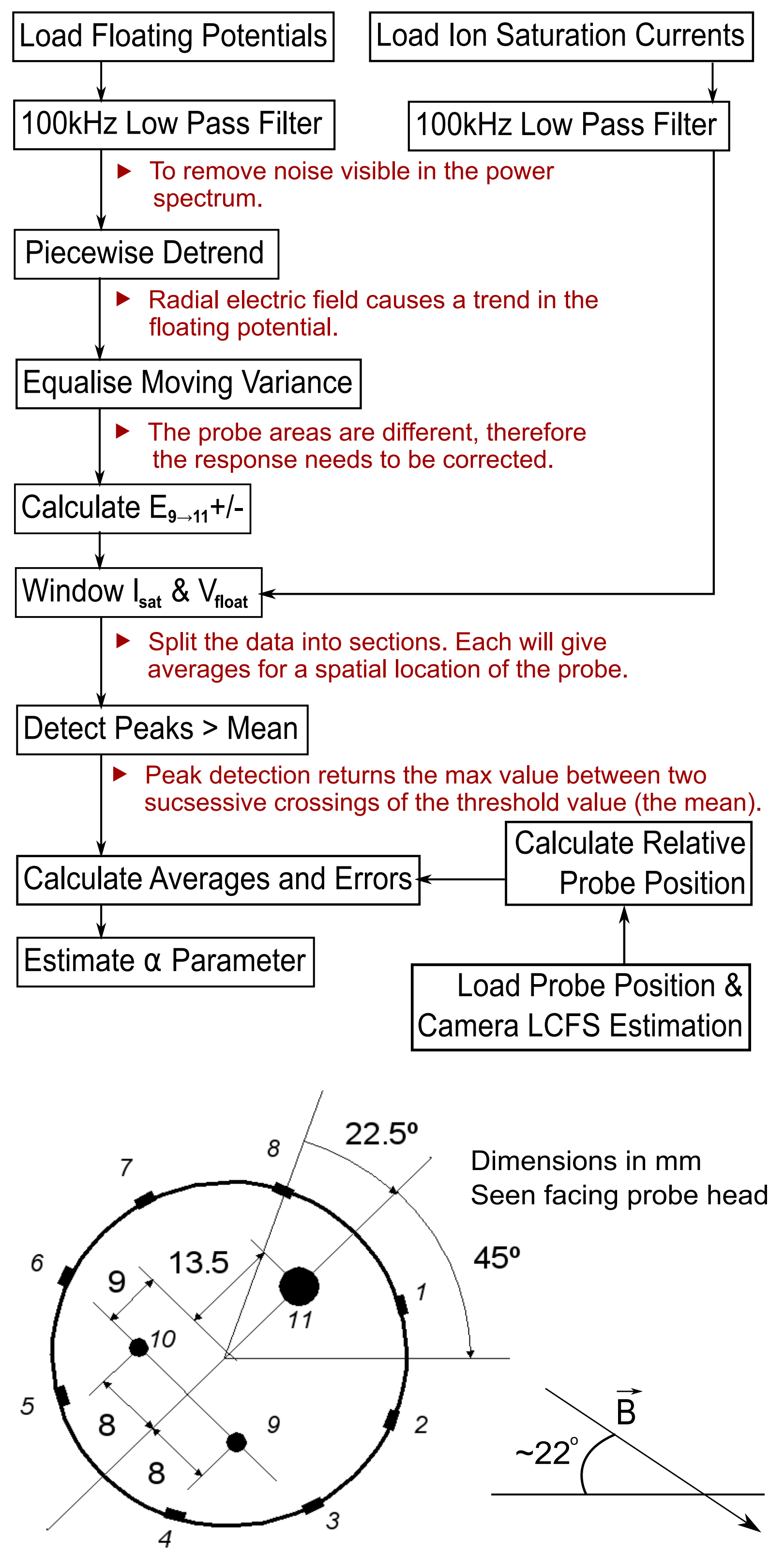
Load Floating Potentials

Load Ion Saturation Currents

100kHz Low Pass Filter

100kHz Low Pass Filter

- To remove noise visible in the power spectrum.

Piecewise Detrend

- Radial electric field causes a trend in the floating potential.

Equalise Moving Variance

- The probe areas are different, therefore the response needs to be corrected.

Calculate $E_{9\rightarrow 11}$+/-

Window $I_{sat}$ & $V_{float}$

- Split the data into sections. Each will give averages for a spatial location of the probe.

Detect Peaks > Mean

- Peak detection returns the max value between two sucsessive crossings of the threshold value (the mean).

Calculate Averages and Errors

Calculate Relative Probe Position

Estimate α Parameter

Load Probe Position & Camera LCFS Estimation

*Analytical process flowchart and probe pinout diagram*

### Scaling of velocity with density

Given the results for sheath dissapative and nonlinear interchange drive filament velocities, the scaling of density with velocity from experiments can be investigated. [**5**]

$$\frac{v_r^{\mathrm{high}}}{v_r^{\mathrm{low}}} \sim \left(\frac{n^{\mathrm{high}}}{n^{\mathrm{low}}}\right)^{\alpha} \tag{1}$$

With $\alpha = 1$ and $\alpha = 0.5$ for linear sheath and nonlinear interchange scalings respectively. This previously applied to a higher and lower density discharge, but is also valid for the direct comparison of individual blobs.

### Correlations

- Correlations between Isat and Vfloat are low.
- Correlations between the floating potentials remain high; a simple formulation of the electric field should be possible.

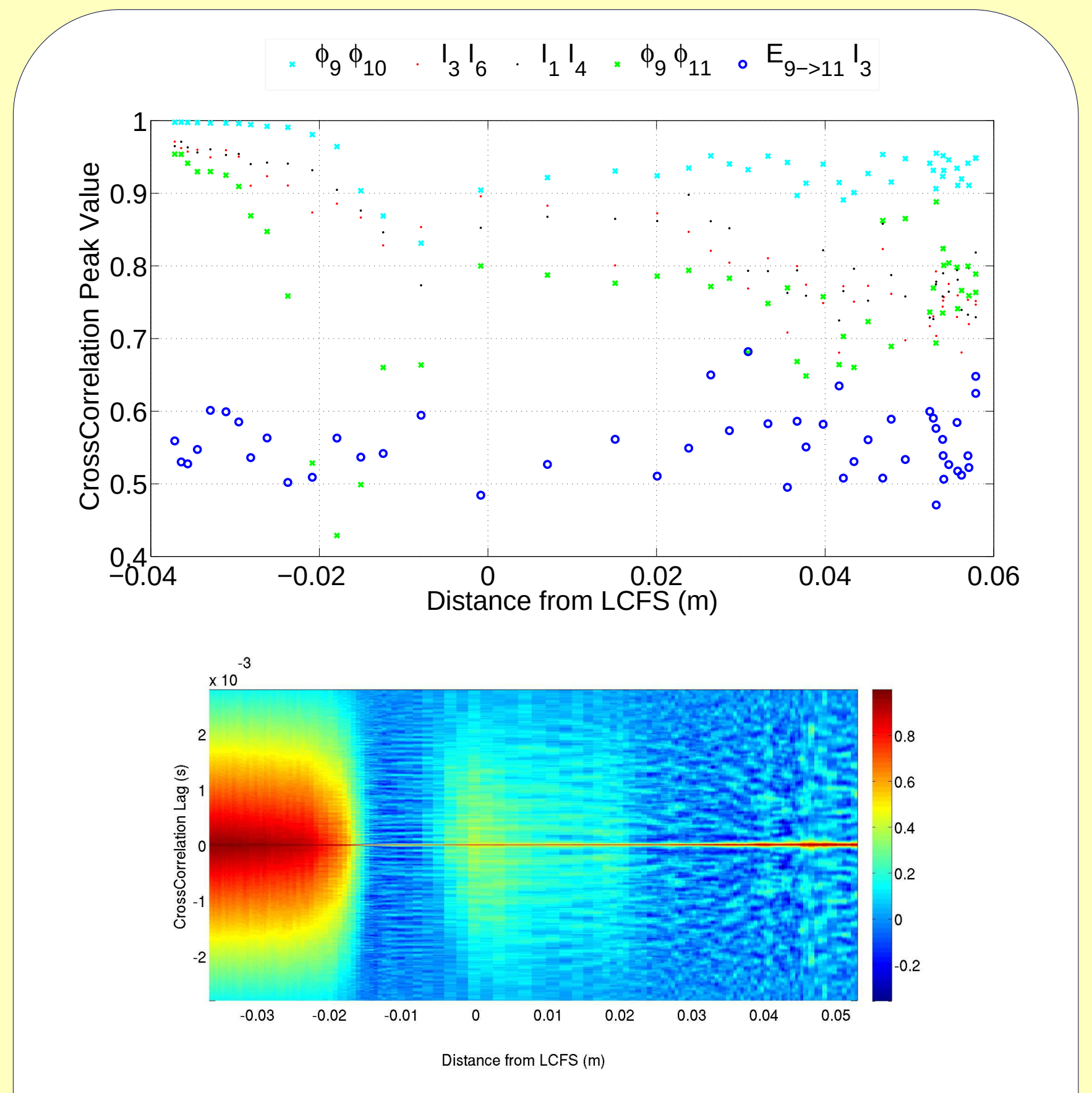

*Top: Peak of cross correlation for various signals vs radius.*

*Below: Crosscorrelation of field-aligned potentials, indicating a possible more remote LCFS than given by $D_\alpha$ emission cameras.*

### Method of obtaining the scaling

- A Bayesian technique is proposed.
- Sets of ion saturation current peaks and electric field peaks will be used in a windowing technique.
- The averages of these sets will be used to find the $\alpha$ parameter.
- The error on the mean is estimated using central limit theorem (i.e as $\frac{\sigma}{N}$).

### Result for $\alpha$

- The result for the scaling parameter is given for positive and negative velocity/density peaks seperately.
- Presumably outward pulses correspond to the density peaks, inward pulses correspond to subdensity peaks [6].

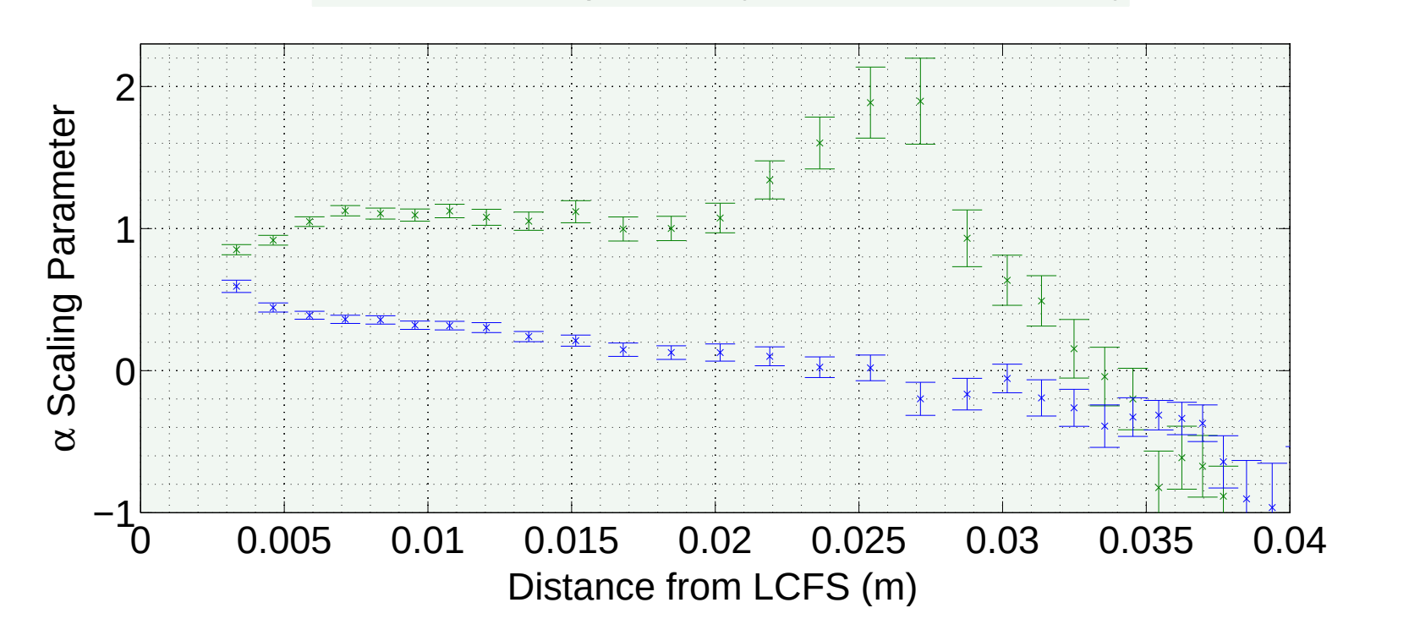

*The alpha exponent (1) for MAST data. LFCS shifted 0.01m inwards, see correlations figure.*

- A tendancy toward polarisation current driven behaviour in the vincinity of the LCFS is seen.
- There is a laregely unpredicable behavour for the filaments at other radial locations.

### Scaling of Absolute Moments for $I_{sat}$

- This method of comparison between structure functions can indicate the presence of types of stochastic behaviour.
- In the vincinity of the LCFS, this shows us a tendancy toward more coherent behaviour in the $I_{sat}$ data.

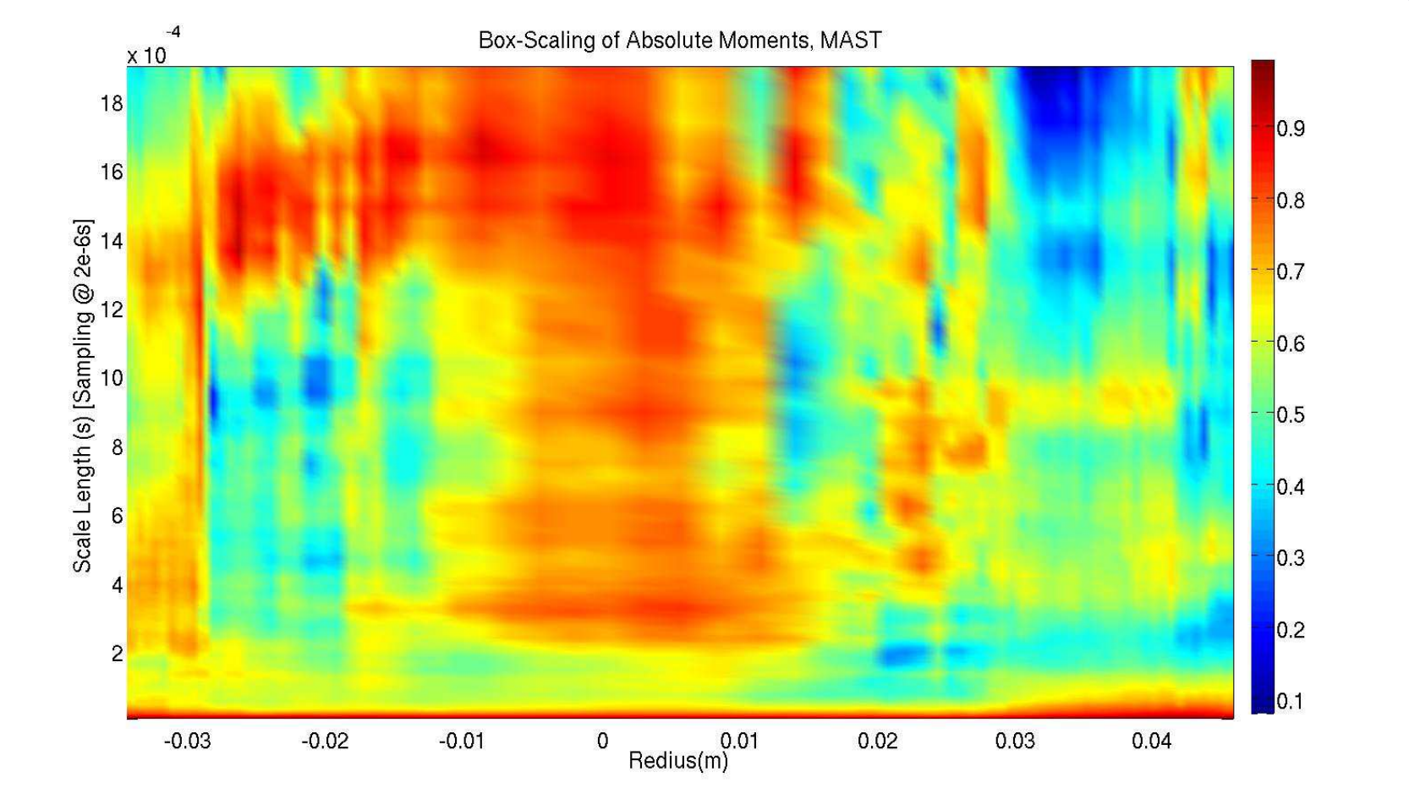

## Simulation

- The interchange scaling result from probe data is compared to a simulation of SOL plasma, from an adaption of the the TOKAM [**6**] code.
- It is a fully nonlinear simulation without the $n = n_0 + \tilde{n}$ local approximation.
- It includes the effects of the Polarisation, Diamagnetic and Sheath currents discussed.

### Numerical Scheme

- Implimented via Runge Kutta Explicit 4th order scheme with 5th order timestep adaption.
- Poisson equation solved spectrally using the MPI FFTW transforms.

### Equations

$$(\partial_t - D\nabla_{\perp}^2)n = [n,\phi] - \sigma n e^{\Lambda-\phi} + S$$

$$g\frac{\partial_y n}{n} + (\partial_t - \mu\nabla_{\perp}^2)\nabla_{\perp}^2\phi = [\nabla_{\perp}^2\phi,\phi] + \sigma e^{\Lambda-\phi}$$

The simulation was ran with $g = 3 \times 10^{-2}$ and $\sigma = 3 \times 10^{-4}$, consitant with the MAST L-mode discharge case

### Scaling of $\alpha$

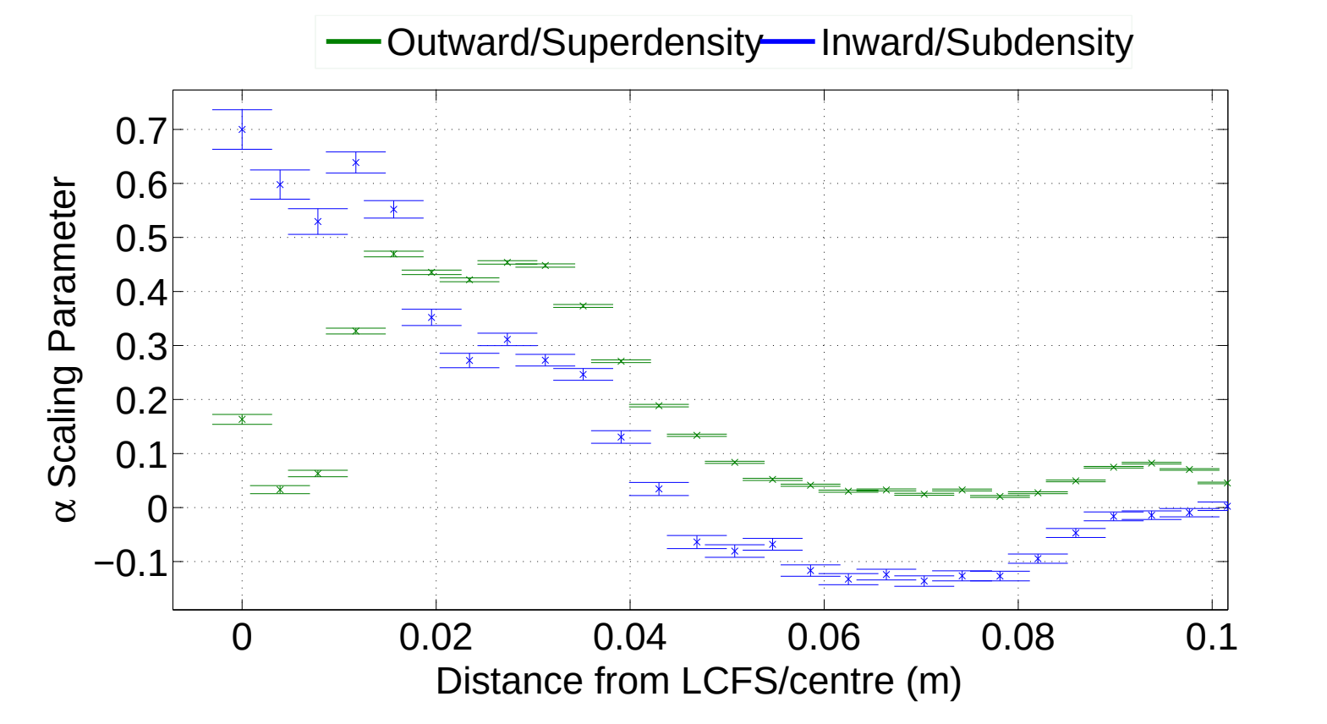

*The alpha exponent (1) for TOKER simulation data.*

- Simulation data analysed using same method as Experimental data.
- Data windowed via peak detections for each radial section.

## References

1. Loarte, A. et al., ITER Physics Basis, Nucl. Fusion 39, 2391
2. Umansky, M. V. et al., Phys. Plasmas 5, 3373
3. Krasheninnikov, S. I. Phys. Lett. A 283, 368
4. O. E. Garcia et al., Phys. Plasmas 13, 082309
5. N. B. Ayed, Doctoral Thesis, University of York, England, 2009
6. Y. Sarazin and Ph. Ghendrih, Phys. Plasmas 5, 12, 4214
7. K.-U. Riemann, Contrib. Plasma Phys., 32, 3/4, 231 (1992)
8. D A Mendis 2002 Plasma Sources Sci. Technol. 11 A219